Bull. Mater. Sci., Vol. 34, No. 7, December 2011, pp. 1483–1489. © Indian Academy of Sciences.

Effect of Zr on dielectric, ferroelectric and impedance properties of $BaTiO_3$ ceramic

SANDEEP MAHAJAN[1,3], O P THAKUR[1], CHANDRA PRAKASH[2,*] and K SREENIVAS[4]

[1]Electroceramics Group, Solid State Physics Laboratory, Lucknow Road, Delhi 110 054, India
[2]Directorate of Extramural Research & Intellectual Property Rights (ER&IPR), DRDO Bhawan, New Delhi 110 105, India
[3]Present address: Department of Physics, Indian Institute of Technology, Delhi 110 016, India
[4]Department of Physics and Astrophysics, University of Delhi, Delhi 110 007, India

MS received 11 April 2010

Abstract. A polycrystalline sample of Zr-doped barium titanate ($BaTiO_3$) was prepared by conventional solid state reaction method. The effect of Zr (0·15) on the structural and microstructural properties of $BaTiO_3$ was investigated by XRD and SEM. The electrical properties (dielectric, ferroelectric and impedance spectroscopy) were measured in wide range of frequency and temperature. With substitutions of Zr, the structure of $BaTiO_3$ changes from tetragonal to rhombohedral. Lattice parameters were found to increase with substitution. The room temperature dielectric constant increases from ~ 1675 to ~ 10586 and peak dielectric constant value increases from ~ 13626 to ~ 21023 with diffuse phase transition. Impedance spectroscopy reveals the formation of grain and grain boundary in the material and found to decrease with increase in temperature.

Keywords. BZT; dielectric; impedance; diffuse phase transitions.

1. Introduction

Since the discovery of barium titanate, $BaTiO_3$, in polycrystalline form, it has been widely used in various electronic components, such as multilayer capacitor (MLCs), positive temperature coefficients of resistivity (PTCR) thermistor, piezoelectric device, optoelectronic components and semiconductors (Morrison *et al* 2001; Weber *et al* 2001; Mahajan *et al* 2009). For MLCs applications, dielectric materials need to be electrically insulating ($>10^{10}$ Ω cm and exhibit high permittivity values (> 1000) at room temperature (Morrison *et al* 2001). Useful properties for commercial device applications have been mostly observed originally in lead-based perovskite compounds such as PMN–PT, PNN–PZT, PLZT and PZT (Park and Shrout 1997; Fu and Cohen 2000; Mahajan *et al* 2009). These compositions have an obvious disadvantage of volatility and toxicity of 'lead'. Manufacturers are now being refrained from using materials especially those containing lead. Therefore, in recent years, research efforts have been directed more towards the development of environmental friendly 'lead-free' compositions.

The solid solution of $BaTiO_3$ and $BaZrO_3$ has been established as one of the most important compositions for dielectric in multilayer capacitors. The high permittivity of $BaTiO_3$ ceramic is enhanced further by the addition of zirconium and meets the Z5U specification of MLCs (Weber *et al* 2001, Tang *et al* 2004; Maiti *et al* 2006a, b). The Zr^{4+} ion (0·72 Å) is chemically more stable than the Ti^{4+} (0·60 Å) and has a larger ionic radius that expands the perovskite lattice. Therefore, BZT material exhibits several interesting features in the dielectric behaviour. The nature of the ferroelectric phase transition at the Curie temperature (T_c) of BZT ceramic changes strongly with Zr content. At higher Zr content (> 0·08), BZT ceramic shows a broad dielectric constant peak near T_c, which is caused by inhomogeneous distribution of Zr ions on Ti sites and mechanical stress in the grain. As the Zr content increases, the phase transition temperatures approach each other, until, at a Zr content of ~ 0·13, only one structural phase transition exists. Below T_c, the rhombohedral phase is stable and, above T_c, cubic. Despite the high dielectric constant value of BZT ceramic, its piezoelectric and impedance properties are less studied in the literature. To further understand the grain and grain boundary effects in these ceramics, the temperature and frequency dependence of electrical and dielectric properties at high temperatures (30 to 600°C) have been studied using complex impedance spectroscopy technique. The frequency-dependent electrical properties are correlated with microstructural changes using appropriate equivalent circuits that match the observed electrical response in complex impedance spectrum.

*Author for correspondence (cprakash@hqr.drdo.in)

2. Experimental procedure

The stoichiometric ratio of starting chemicals $BaCO_3$ (99·9%), TiO_2 (99·9%) and ZrO_2 (99·9%) (Aldrich Chemical) were weighed for the composition $BaZr_xTi_{1-x}O_3$ ($x = 0$ and 0·15). The weighed powders were wet ball milled for 24 h using high-density zirconia balls and distilled water as wetting media. After drying, calcination was done in high-purity alumina crucibles at 1200°C for 6 h in a conventional furnace. The calcined powder was again ball-milled for about 24 h, dried and then sieved. The sieved powders were pressed into rod form at a pressure of 200 MPa using a Cold Isostatic Press (M/s Autoclave Engineers, USA). Rods were sintered at 1400°C for 6 h with 3°C/min heating and cooling rate. The phase purity of the compound was confirmed by X-ray diffraction (XRD) technique. XRD analysis of the sample was carried out using Philips Diffractometer model PW-3020 with Cu-Kα ($\lambda = 1{\cdot}5418$ Å) radiation in a wide range of 2θ ($20° < 2\theta < 80°$) at scanning rate of 2°/min. Density and microstructural information was obtained by the Archimedes principle and SEM (Leo 1430, Japan), respectively. For electrical measurements, slices (cut from rods) of dimension 0·5 mm thickness and 8 mm diameter were prepared. Both the sides of slices were properly polished, cleaned and gold sputtered for making the electrode using Sputter Coater (Desk II TSC Cold Sputter/ Etch Unit). Measurements of capacitance (C), dissipation factor (tan δ) and impedance/admittance on ceramic discs as a function of frequency (40 Hz–1 MHz) and temperature (523–873 K) were carried out using an Agilent 4294A Impedance analyser interfaced with a PC. P–E hysteresis loops were recorded using automated P–E loop tracer (M/s AR Imagetronics, India) at 50 Hz based on modified Sawyer-Tower circuit. The remnant polarization (P_r) and coercive field (E_c) were determined from the hysteresis loops and strain was measured using a SS50 strain measurement system (Sensor Tech., Canada).

3. Results and discussion

3.1 *Structural properties*

Phase formation of the prepared samples was confirmed by XRD technique. XRD pattern of $BaZr_{0·15}Ti_{85}O_3$ (BZT15) (figure 1b) ceramic, suggesting there is change in peak position as compared to pure $BaTiO_3$ (BT) (figure 1a). It can be seen that with Zr substitution in $BaTiO_3$, the 2θ peaks shifted towards lower angle side, indicating increase in the value of lattice parameter. This is because of the ionic radius of Zr^{4+} (0·72 Å) is large as compared to Ti^{4+} (0·60 Å). Lattice parameter and lattice volume are calculated using PowderX software. The analysis shows tetragonal and rhombohedral structure for pure BT and BZT15, which supports the earlier reports on BZT (Yu *et al* 2000a). The experimental density is measured by Archimedes principle and with the help of unit cell volume, theoretical or X-ray density (d_{th}) was calculated using the relation

$$d_h = \left(\frac{Z{\cdot}M}{N{\cdot}V}\right)_{g/cc}, \quad (1)$$

where Z is the number of molecules in a unit cell and is equal to 1 for the present system, M is the molecular weight of the compound, N is the Avogadro's number and V is the volume of unit cell. Both the samples are found to be dense and table 1 shows the values of experimental density and lattice parameters.

Figure 2 represents the microstructure of thermally etched ceramic samples for $x = 0$ and 0·15. Average grain size was measured by linear intercept method and given in table 1. It can be seen from the micrographs that the Zr ion substitution has a strong effect on the grain size and its value decreases from 11·5 to 1·9 μm.

3.2 *Dielectric properties*

Figure 3(a and b) shows the frequency dependence of dielectric constant and tan δ at room temperature for pure BT and BZT15 ceramic samples, respectively. It can be seen that the value of dielectric constant is higher at lower frequency and with increase in frequency, it decreases because in a dielectric material, polarization occurs due to contributions of electronic, ionic, dipolar and space charge region. At lower frequencies, all the types of polarization contribute to polarization and as the frequency increases, contribution of different polarization

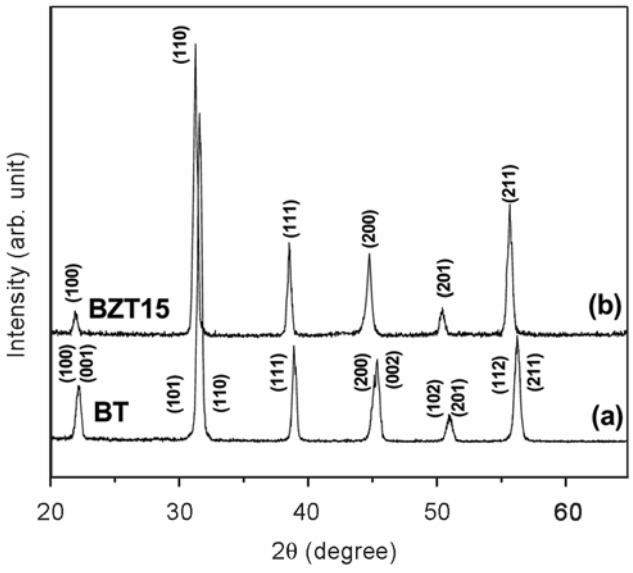

Figure 1. X-ray diffraction patterns for (a) $BaTiO_3$ and (b) $x = 0{\cdot}15$ doped Zr.

Table 1. Structural parameters of $BaZr_xTi_{1-x}O_3$ (x = 0 and 0·15) ceramic samples.

Compound	Exp. density (g/cc)	$\alpha°$	Lattice parameter and structure (Å)				Volume $(Å)^3$	Densification (%)	Average grain size (μm)
				(*a*)	(*b*)	(*c*)			
BT	5·65	90·00	Tetra.	3·9848	3·9848	4·0162	63·77	78·5	11·5
BZT15	5·93	89·62	Rhom.	4·0429	4·0429	4·0429	66·08	83·1	1·9

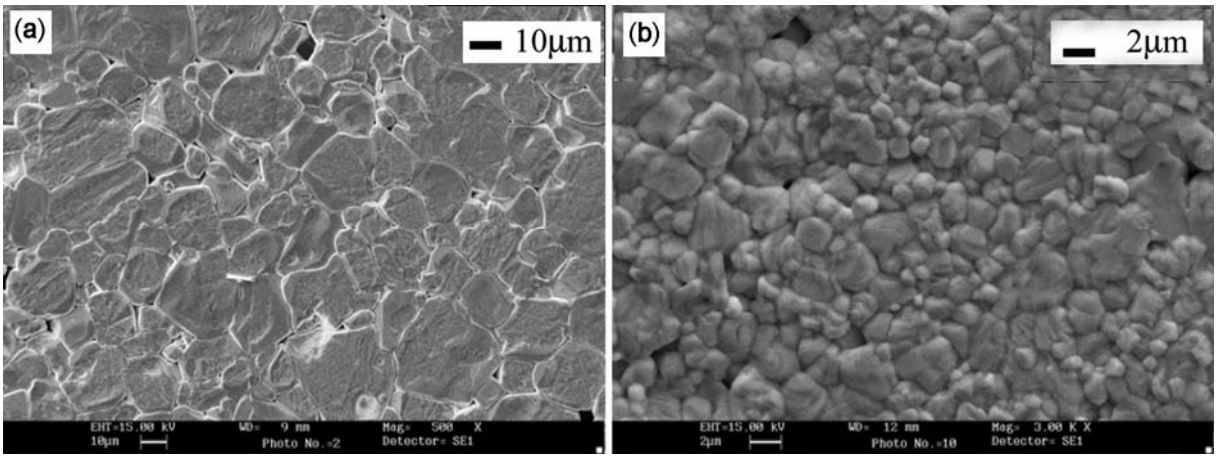

Figure 2. Scanning electron micrograph for (**a**) $BaTiO_3$ and (**b**) BZT15.

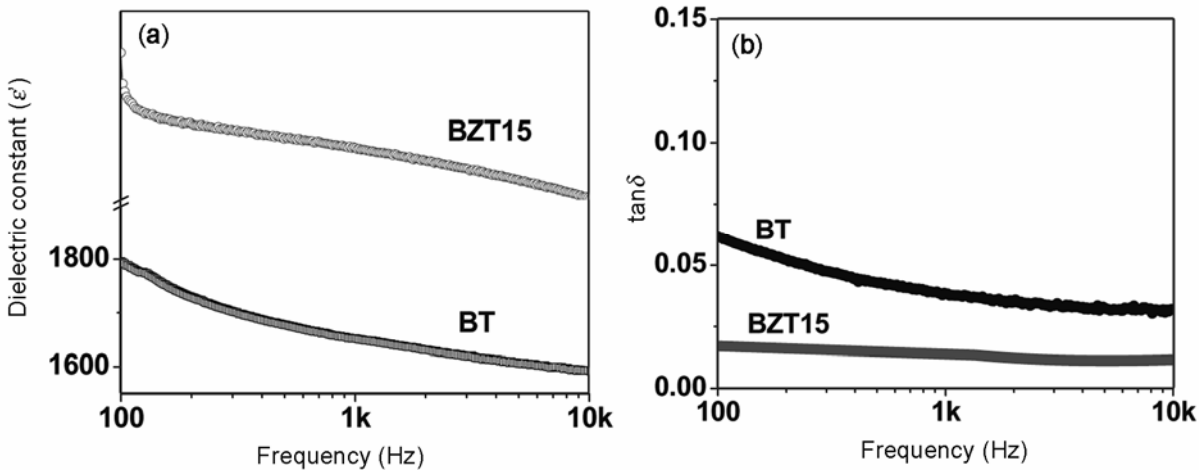

Figure 3. Variation of (**a**) dielectric constant and (**b**) tan δ for $BaTiO_3$ and BZT15 as a function of frequency.

decreases and at higher frequency only dipolar and electronic polarization mainly contributes to polarization (Moulson *et al*). These figures also reveal that the room temperature dielectric constant value increase from 1675 to 10586 with Zr = 0·15 at 1 kHz as compared to pure BT.

Figure 4(a and b) shows the variation in the dielectric constant of pure BT and BZT15 ceramic sample as a function of temperature in the frequency range of 100 Hz to 500 kHz. Both the samples show an increase in dielectric constant with temperature, reaching to maximum, and then decrease with further increase in temperature, which is a typical characteristic of ferroelectrics.

For $BaTiO_3$ (figure 4a) we observed three different phase transitions at 120°C, 5°C and –90°C, which is well supported by earlier results (Jaffe *et al* 1971), the first is the paraelectric to ferroelectric phase transition, i.e. T_m or (T_c), which occurs at ~ 120°C, the second is a ferroelectric to another ferroelectric transition in which the structure changes from tetragonal to orthorhombic (T_1) at 5°C and the third one is again ferroelectric to ferroelectric (T_2) at –90°C and the structure changes from orthorhombic to

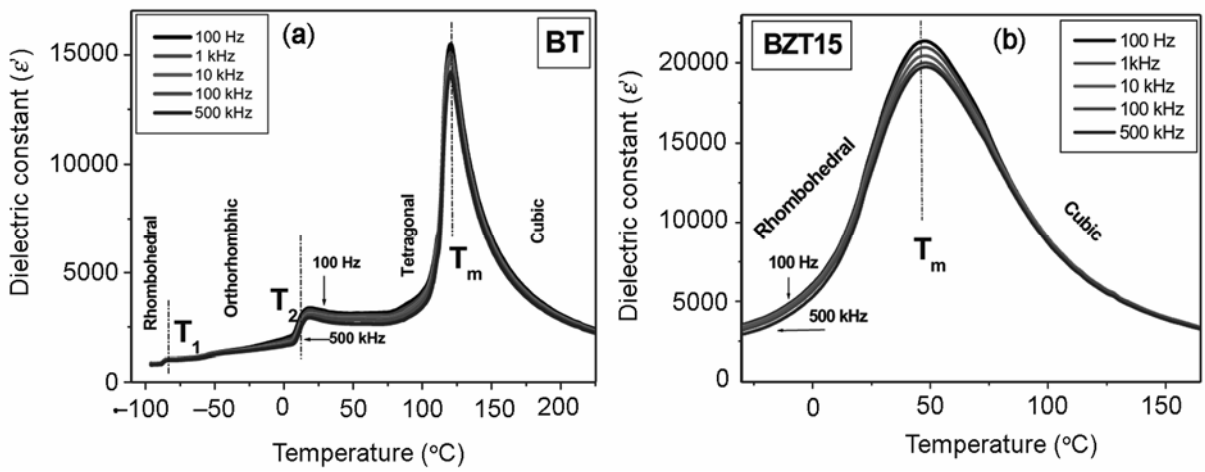

Figure 4. Temperature variation of ε' different frequencies for $BaZr_xTi_{1-x}O_3$ ceramic sample with (**a**) $x = 0$ and (**b**) 0·15.

Table 2. Ferroelectric and piezoelectric properties of $BaZr_xTi_{1-x}O_3$ ($x = 0$ and 0·15) ceramic samples.

	P–E loop			
Compound	Pr (μC/cm^2)	E_c (kV/cm)	Strain (%)	Degree of hysteresis $\Delta x/x$ (%)
BT	5·45	3·14	0·08	25·4
BZT15	1·45	0·20	0·05	0·9

rhombohedral (Jaffe *et al* 1971; Hennings *et al* 1982). Additions of Zr strongly influence the phase-transition temperature, shifting them towards lower temperatures ~ 48°C. Because of the larger radius of Zr^{4+} (0·72 Å), its substitution in Ti^{4+} (0·60 Å) may depress the oriented displacement of the B-site ions in the oxygen octahedra. Therefore, the interactions between the B-site ions and O^{2-} would become weaker, resulting in a decrease in phase-transition temperature (Sawangwan *et al* 2009; Tang *et al* 2004).

The value of dielectric constant in the present study is very close to, or in some cases higher than that of the single crystal grown by laser-heated pedestal technique by Yu *et al* (2000). The same composition synthesized by Wang *et al* (2002) showed a lesser value of peak dielectric constant (~ 8500) as compared to this study (~ 21023); the reason may be because of better densification of our sample.

The dielectric constant of a normal ferroelectric in paraelectric region generally follows the Curie–Weiss law described by

$$\frac{1}{\varepsilon'} = \frac{(T - T_0)}{C} \quad (T > T_m), \tag{2}$$

where T_0 is the Curie temperature, C is Curie–Weiss constant and T_m is the Curie point or transition temperature. However, in substituted ferroelectric like PMN, deviation from the Curie–Weiss behaviour has been observed. It is seen that the Zr-substituted ceramic does not follow the Curie–Weiss law, and therefore we applied a modified Curie–Weiss law, which was proposed by Uchino and Nomura (1982) to describe the diffuseness of the phase transition as

$$\frac{1}{\varepsilon'} - \frac{1}{\varepsilon'_m} = \frac{(T - T_m)^\gamma}{C_1} \quad (T > T_m), \tag{3}$$

where γ and C_1 are modified constants, with $1 < \gamma < 2$. The value of the parameter γ gives information about the character of the phase transition. The value of γ is 1 for the case of a normal ferroelectric and a quadratic (i.e. $\gamma = 2$) is valid for a relaxor with diffused ferroelectric (Smolenski *et al* 1958; Ang *et al* 2002; Victor *et al* 2003). Figures 5(a and b) represents the plot of $\log(1/\varepsilon' - 1/\varepsilon'_m)$ vs. $\log(T - T_m)$ for pure $BaTiO_3$ and Zr-substituted BZT15, in which symbols denote experimental data and solid line denotes fitting to the modified Curie–Weiss law. It is observed that the value of the diffusive parameter increases from 1·25 to 1·82.

3.3 *Ferroelectric and piezoelectric properties*

Figure 6 represents the room temperature hysteresis loop of $BaTiO_3$ and the inset represents the BZT15 ceramic sample. A well-saturated shape typical of ferroelectric materials was evident for both the compositions. The values of

Table 3. Resistance (R_g, R_{gb}) and capacitance (C_g, C_{gb}) of grains and grain boundaries of BZT15 ceramics.

Temperature (°C)	R_g (kΩ)	R_{gb} (kΩ)	C_g (pF)	C_{gb} (nF)
425	480	1870	0·31	1·99
450	320	960	0·29	1·88
475	220	570	0·28	1·83
500	160	350	0·27	1·76
525	110	230	0·26	1·71

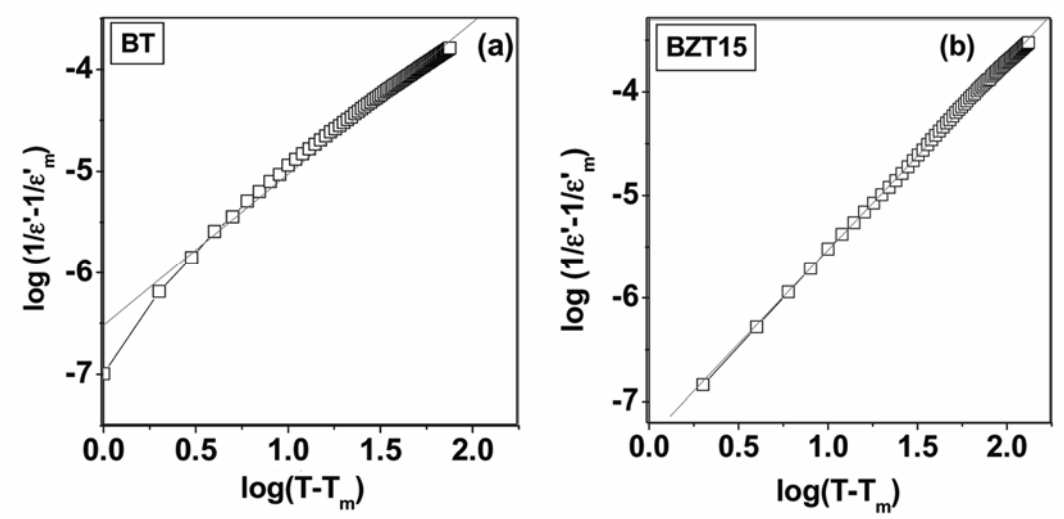

Figure 5. Plot of $\log(1/\varepsilon' - 1/\varepsilon'_m)$ vs $\log(T - T_m)$ for $BaZr_xTi_{1-x}O_3$ for (**a**) $x = 0$ and (**b**) 0·15.

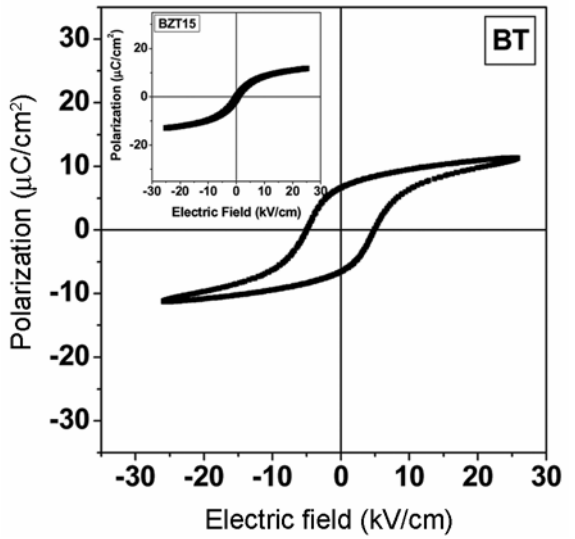

Figure 6. Polarization vs electric field (P–E) hysteresis loop of $BaZr_xTi_{1-x}O_3$ ceramic with (**a**) $x = 0$ and (**b**) 0·15.

remnant polarization (P_r) and coercive field (E_c) are calculated from the loop and are summarized in table 2. It can be seen that for pure $BaTiO_3$, P_r is 5·45 μC/cm^2 with E_c of 3·14 kV/cm, and with substitutions of Zr, $x = 0{\cdot}15$, it decreases to 1·45 μC/cm^2 while its coercive field decreases to 0·20 kV/cm.

Similarly, figure 7 represents the strain electric field behaviour of pure BT and BZT15. Although with Zr concentration, the strain level is decreased significantly, at the same time the degree of hysteresis (which is the ratio of the strain deviation during the rise and fall with the field (Δx at half of the maximum field (20 kV/cm) divided by the maximum strain x_{max} at 40 kV/cm) is found to decrease from 25·4 to 0·9. The values of $\Delta x/x$ are listed in table 2. These results on reduced hysteresis indicate the usefulness of the ceramics processed in the present study for potential application as positioning actuators.

The decrease in strain with increase of Zr can be correlated with the observed finer grain size and microstructure. Yamaji *et al* (1977) reported a fine grain structure (1·5 μm) in Dy-doped fine BT in comparison to the undoped coarse grain ceramic of (50 μm) in $BaTiO_3$. According to their results, as the grains become finer, under the same electric field, the absolute value of strain decreases and the hysteresis becomes smaller. This is because of increase in the coercive field for 90° domain rotation with decreased grain size.

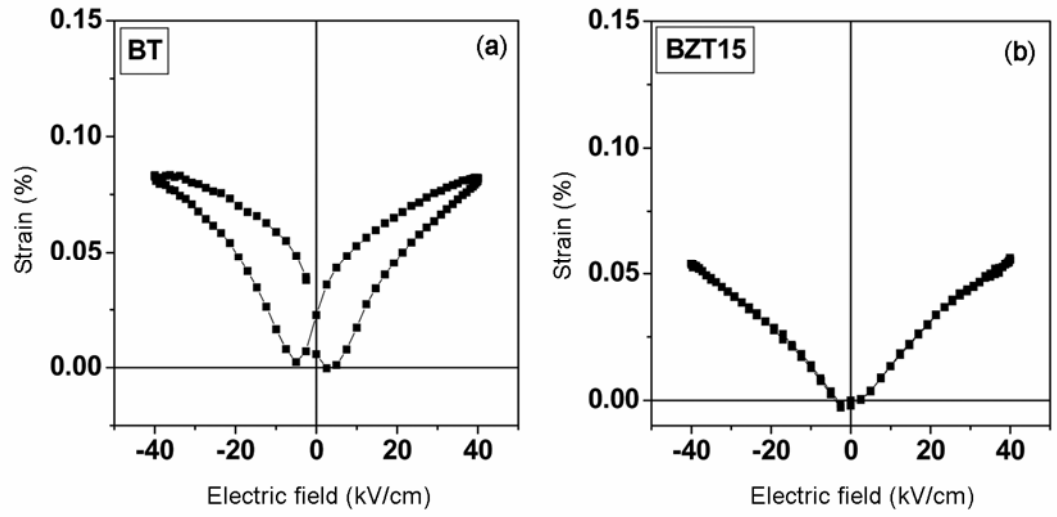

Figure 7. Strain vs electric field (*S–E*) loop of $BaZr_xTi_{1-x}O_3$ ceramic with (**a**) $x = 0$ and (**b**) 0·15.

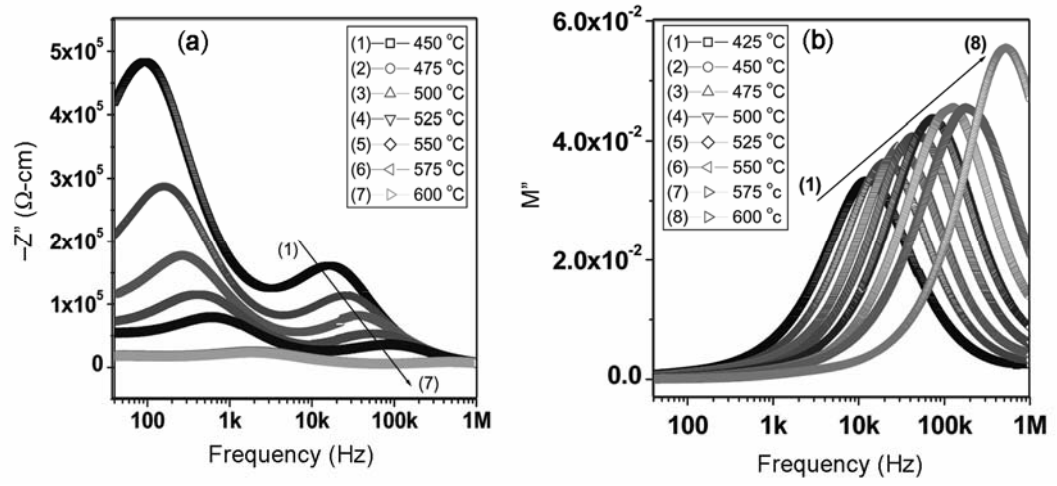

Figure 8. Frequency dependence of imaginary part of (**a**) impedance Z'' and (**b**) modulus M'' at different temperatures for BZT15 ceramic sample.

3.4 *Impedance spectroscopy*

Figure 8(a and b) represents the variation of imaginary part of impedance (Z') and modulus as a function of frequency at different temperatures for BZT15 ceramic. In the lower frequency side, normal variations in Z'' values with temperature and frequency were observed and all the curves at different temperatures appear to merge in to a single curve in the higher frequency region (figure 8a). The appearance of Z'' peak at a characteristic frequency ($\omega_{max} = 2\pi f_{max}$) is also found to depend on temperature, and could be related to the type and strength of the electrical relaxation phenomenon in the material (Pastor *et al* 2007). As the temperature increases, two peaks at different frequency regions and at different temperatures are distinctly observed and shifted towards higher temperature side with increase in temperature. The low frequency region peak corresponds to grain boundary, while higher frequency region peak represents the bulk (grain) contribution. As the temperature increases, the value of Z'' decreases, indicating a decrease in the resistive nature of the sample (Sen *et al* 2004). In order to separate the *RC* element and determine their components *R* and *C* values, analysis using both impedance and electric modulus formalism was employed (Sinclair *et al* 1989; Hirose *et al* 1996; Mahajan *et al* 2009). The value of resistance and capacitance for grain and grain boundary were obtained using the relation $2\pi f_m RC = 1$ from Z'' vs log$f$ plot and simulated by using '*Zview*' software (West *et al* 2004). It is observed that two parallel *RC* contributions, in series with each other, are found to best fit the experimental data very well, indicating contributions from grain and grain boundary in the samples.

The figure 8b shows the plot of imaginary part M'' with frequency at different temperatures. The use of modulus spectroscopic plot is particularly useful for separating

component with similar resistance but different capacitance. In figure 8b, peaks appear to be shifted towards higher frequency side with rise in temperature. It is also observed that M'' peaks broaden with decrease in temperature. The observed temperature and frequency dependence of M'' arises due to distribution of relaxation time in the sample. The values of grain resistance (R_g), grain boundary resistance (R_{gb}), grain capacitance (C_g) and grain boundary capacitance (C_{gb}) are shown in table 3, which indicates that R_{gb} is more resistive in nature as compared to R_g and, similarly, the value of C_{gb} is higher compared to C_g at all temperatures. The decrease in both grain and grain-boundary resistance with increasing temperature indicates a negative temperature coefficient of resistance (NTCR) behaviour (Zhang *et al* 2004).

4. Conclusions

Zr-doped $BaTiO_3$ ceramics prepared through conventional solid state reaction method shows single phase perovskite at room temperature with rhombohedral structure. Addition of Zr increases room temperature and peak dielectric constant values, which can be useful for dielectric for capacitor application. Degree of hysteresis reduces from 25·4% to 0·9% with substitution. Impedance and modulus spectroscopy reveals the presence of grain and grain boundary contribution in the sample.

Acknowledgements

The authors would like to thank Mr Anshu Goyal of SSPL, Delhi, for XRD measurements and Mr Pathaniya of AIIMS, New Delhi, for SEM measurements.

References

Ang C, Jing Z and Yu Z 2002 *J. Phys Condens. Matter* **14** 8901

Fu H and Cohen R E 2000 *Nature* (*London*) **403** 281

Hennings D, Schnell A and Simon G 1982 *J. Am. Ceram. Soc.* **65** 539

Jaffe B, Cook W R and Jaffe H 1971 *Piezoelectric ceramics* (New York: Academic Press) Ch. 1, pp 1–5

Mahajan S, Thakur O P and Prakash C 2009 *J. Alloy Compds* **471** 507

Mahajan S, Thakur O P, Bhattacharya D K and Sreenivas K 2008 *Mater. Chem. Phys.* **112** 858

Mahajan S, Thakur O P, Bhattacharya D K and Sreenivas K 2009 *J. Am. Ceram.. Soc.* **92** 416

Maiti T, Guo R and Bhalla A S 2006a *Appl. Phys. Lett.* **100** 114109

Maiti T, Guo R and Bhalla A S 2006b *Appl. Phys. Lett.* **89** 122909

Morrison F D, Sinclair D C and West A R 2001 *Inter. J. Inorg. Mater.* **3** 1205

Moulson A J and Herbert J M *Electroceramics: materials, properties and application* (London, UK)

Park S E and Shrout T R 1997 *J. Appl. Phys.* **82** 1804

Pastor M, Bajpai P K and Choudhary R N P 2007 *J. Phys. Chem. Solids* **68** 1914

Sawangwan N, Barrel J, Mackenzie K and Tunkasiri T 2008 *Appl. Phys.* **A90** 723

Sinclair D C and West A R 1989 *J. Appl. Phys.* **66** 3850

Smolenski G A and Agranovskaya A I 1958 *Sov. Phys. Tech. Phys.* **3** 1380

Tang X G, Chew K H and Chan H L W 2004 *Acta Mater.* **52** 5177

Victor P, Ranjith R and Krupanidhi S B 2003 *J. Appl. Phys.* **94** 7702

Wang Y, Li L, Qi J and Gui Z 2002 *Ceramic Inter.* **28** 657

West A R, Adams T B, Morrison F D and Sinclair D C 2004 *J. Euro. Ceram. Soc.* **24** 1439

Yamaji A, Enomoto Y, Kinoshita K and Tanaka T 1977 *Proc. 1st Mtg. Ferroelectric Mater. & Appl.* Kyoto 269

Yu Z, Guo R and Bhalla A S 2000a *J. Appl. Phys.* **88** 410

Yu. Z, Guo R and Bhalla A S 2000b *Appl. Phys. Lett.* **77** 1535

Zhang R, Li J F and Viehland D 2004 *J. Am. Ceram. Soc.* **87** 864